Materials Today Bio 24 (2024) 100906

Contents lists available at ScienceDirect

Materials Today Bio

journal homepage: www.journals.elsevier.com/materials-today-bio

A multifunctional quercetin/polycaprolactone electrospun fibrous membrane for periodontal bone regeneration

Yue Hu [a,b,c,1], Zeyu Fu [b,c,d,e,1], Shiyuan Yang [a,b,c,1], Yuning Zhou [a,b,c], Huimin Zhu [a,b,c], Yan Zhu [a,b,c], Jia Zhou [a,b,c], Kaili Lin [b,c,d,f,**], Yuanjin Xu [a,b,c,*]

[a] Department of Oral Surgery, Shanghai Ninth People's Hospital, Shanghai Jiao Tong University School of Medicine, Shanghai, China
[b] College of Stomatology, Shanghai Jiao Tong University, Shanghai, China
[c] National Center for Stomatology, National Clinical Research Center for Oral Diseases, Shanghai Key Laboratory of Stomatology, Shanghai Research Institute of Stomatology, Shanghai, China
[d] Department of Oral and Cranio-maxillofacial Surgery, Shanghai Ninth People's Hospital, Shanghai Jiao Tong University School of Medicine, Shanghai, China
[e] School of Materials and Chemistry, University of Shanghai for Science and Technology, Shanghai, China
[f] Research Unit of Oral and Maxillofacial Regenerative Medicine, Chinese Academy of Medical Sciences, Shanghai, China

1. Introduction

Periodontal diseases are chronic inflammatory diseases that mainly affected the periodontal supporting tissues, such as the gingiva, periodontal ligament and alveolar bone, which could ultimately lead to tooth loss. Almost 90 % of the worldwide population suffers from periodontal disease [1]. Periodontal disease was shown to contribute to systemic inflammation of the body and deteriorating conditions, including hypertension, atherosclerosis and diabetes mellitus [2]. Conventional management for periodontal disease such as scaling, root planning, local or systemic application of antibiotics, open flap debridement and guided tissue regeneration (GTR), has been demonstrated to be efficacious [3].

Currently, GTR has been proven to be effective and widely applied in periodontal tissue regeneration. The apical migration of connective tissues and gingival epithelium is prevented or impeded by using GTR membranes, therefore, enabling alveolar bone and periodontal ligament to optionally cover the root surface [4]. Based on the biodegradability of GTR membranes, they can generally be classified into two categories: nonabsorbable membranes and absorbable membranes [5]. Nonabsorbable membranes such as polytetrafluoroethylene (PTFE) and titanium require a second surgery for remove, which may cause infection and trauma to the defect sites. Absorbable membranes consist of naturally derived polymers and synthetic degradable polymers [6]. Naturally derived polymers such as collagen are commonly considered to possess fine biocompatibility and have been extensively applied in clinical practice [7]. Nevertheless, the currently present available GTR membranes still have some shortcomings. Previous studies have shown that the degradation rate of the Bio-Gide collagen membranes reached 60 % at 4 weeks and 80 % at 9 weeks post-operation in calvarial defects of rats [8]. The inappropriate degradation rate and inadequate mechanical properties of the absorbable membranes may give rise to the collapse and shrinkage of the membranes into the defect site, making it difficult to maintain enough space at the defect site. Moreover, currently available absorbable membranes mainly exert a barrier function during GTR procedures, while they have limited ability in promoting periodontal tissue regeneration [4]. Therefore, it is of critical importance to devise improved GTR membranes with excellent mechanical properties, appropriate degradation rates, good biocompatibility and the ability to induce osteogenic differentiation of PDLSCs.

Quercetin is a naturally derived dietary polyphenol that is abundantly available in numerous fruits and vegetables [9]. Previous studies have reported that quercetin possess many pharmacological properties, such as anti-inflammatory, antioxidant and osteogenic properties [10–12]. In particular, quercetin could promote the osteogenic differentiation of adipose-derived stem cells *in vitro* [13]. Quercetin could also enhance the osteogenesis under osteoporotic conditions [14]. The incorporation of quercetin in silk fibroin/hydroxyapatite scaffolds was shown to significantly accelerate bone regeneration [15].

Electrospinning is an electrohydrodynamic process in which liquid droplets are electrified to jets, and then, fibers are produced by stretching and elongation [16]. The dimensional structures of electrospun membranes are similar to those of the extracellular matrix (ECM), which can facilitate the proliferation and recruitment of native cells,

* Corresponding author. Department of Oral Surgery, Shanghai Ninth People's Hospital, Shanghai Jiao Tong University School of Medicine, Shanghai, China.
** Corresponding author. College of Stomatology, Shanghai Jiao Tong University, Shanghai, China.
E-mail addresses: lklecnu@aliyun.com (K. Lin), drxuyuanjin@126.com (Y. Xu).
[1] These authors contributed equally to this work.

https://doi.org/10.1016/j.mtbio.2023.100906
Received 29 May 2023; Received in revised form 3 December 2023; Accepted 6 December 2023
Available online 17 December 2023

therefore, promoting regeneration of the tissue [17]. In addition, biomolecules and compounds that possess biological effects can be delivered by electrospun membranes [18]. Polycaprolactone (PCL) is a synthetic polymer with fine biocompatibility, flexibility and biodegradability and has been broadly applied for drug and tissue engineering. Therefore, PCL electrospun fibrous membranes might be suitable candidate GTR membranes for periodontal tissue regeneration.

In this study, we fabricated a flexible Qtn/PCL membrane with reinforced mechanical properties, an appropriate degradation rate, good biocompatibility and an osteogenic induction ability that could promote periodontal tissue regeneration. Quercetin was dispersed in a PCL solution, and fibrous membranes were developed by electrospinning. The physicochemical and biological properties of quercetin/PCL fibrous membranes were evaluated *in vitro*. To further verify the effects of Qtn/PCL fibrous membranes *in vivo*, we established a rat periodontal bone defect model and implanted Qtn/PCL fibrous membranes. The fabricated membranes might provide a new strategy for periodontal tissue regeneration.

2. Materials and methods

2.1. Isolation and identification of hPDLSCs

The experiment was authorized by the Medical Ethical Committee of Shanghai Ninth People's Hospital affiliated to Shanghai Jiao Tong University School of Medicine (SH9H-2022-T370-1). PDLSCs were isolated from patients aged 18–25 years who had premolars or the third molars extracted for orthodontic treatment through the enzyme digestion method [19]. Briefly, the extracted premolars or the third molars were rinsed with phosphate-buffered saline (PBS) containing 5 % penicillin-streptomycin, and the periodontal ligament was gently scraped from the middle of the root surface. Then the periodontal ligament was digested for 1 h in a mixture of dispase (4 mg/mL) (Sigma-Aldrich, D4818, USA) and type I collagenase (3 mg/mL) (Sigma-Aldrich, SCR103, USA) at 37 °C. Finally, the cells were seeded in 10 cm culture dishes with minimum essential medium α (α-MEM) containing 10 % fetal bovine serum (FBS) and 1 % penicillin-streptomycin. PDLSCs from passages 2–4 were used for the following experiments. The identification of PDLSCs was conducted according to the literature [20]. The detailed methods and results were presented in supplementary information.

2.2. Preparation of the electrospun fibrous membranes

Fibrous membranes containing quercetin (Sigma-Aldrich, Q4951, USA) (Qtn) were fabricated by electrospinning [21]. Briefly, PCL (Sigma-Aldrich, 440,744, USA) was dissolved in hexafluoroisopropanol (HFIP) (Macklin, H811026, China) at a final concentration of 16 % (w/v) and stirred on a magnetic stirrer overnight. Next, different amounts of quercetin (0, 0.5 %, 1 %, 2 %, 4 % and 8 wt% of the dissolved PCL) were added to the above PCL solution and oscillated by ultrasound for 30 min to form a homogeneous Qtn/PCL solution. Then the solution was transferred into a 5 mL syringe with a 21 G needle head. Electrospinning was accomplished at a voltage of 10 kV. The supply rate of the solution was 1 mL/h, and with the collecting distance was 25 cm. The whole electrospinning process took 3 h, and the average thickness of the fibrous membranes was approximately 40–70 μm. The membranes containing 0, 0.5 %, 1 %, 2 %, 4 % and 8 wt% quercetin was named as PCL, 0.5%Qtn/PCL, 1%Qtn/PCL, 2%Qtn/PCL, 4%Qtn/PCL and 8% Qtn/PCL, respectively. The membranes were cut into circular shape (diameter of 15 or 34 mm) and sterilized by ultraviolet light for the following experiments [22].

2.3. Characterization of the electrospun fibrous membranes

Scanning electron microscope (SEM) (Zeiss Gemini 300, Germany) was utilized to evaluate the surface morphology of the electrospun fibrous membranes [23]. The average diameters of the fibers were analyzed by Origin 8.0 software. The chemical structures of the electrospun fibrous membranes were assessed by attenuated total reflectance fourier transform infrared spectroscopy (ATR-FTIR) (Thermo Scientific Nicolet iN10, USA) at wavelengths between 500 and 4000 cm^{-1}. Transmission electron microscope (TEM) (JEOL JEM-F200, Japan) was used to analyze the structure of quercetin and the incorporation of quercetin into the fibers.

2.4. Evaluation of tensile mechanical properties

The tensile mechanical properties of the electrospun fibrous membranes were assessed by a universal tester (Hengyi, China) at room temperature [24]. Briefly, all samples were cut into rectangles (6 cm × 3 cm) and the thickness of each sample was measured by a caliper. In this experiment, the crosshead speed was 5 mm/min, and the ultimate tensile strength, Young's modulus, elongation at break and stress-strain curve were recorded or calculated (n = 3).

2.5. Water contact angle analysis

Water contact angles of the electrospun fibrous membranes were analyzed by a contact angle meter (Kruss, Germany) to assess their hydrophilicity [25]. Briefly, 10 μl of the deionized water was dropped on the surface of the electrospun fibrous membranes, and water contact angles were detected (n = 3).

2.6. Cytocompatibility evaluation of the electrospun fibrous membranes

The electrospun fibrous membranes were tailored into circular shapes with diameters of 15 mm, and were placed in the bottom of a 24-well plate. NIH3T3 fibroblasts and hPDLSCs were seeded on the electrospun fibrous membranes at a density of 1 × 10^3 cells/well and 1 × 10^4 cells/well, respectively [26].

After incubation for 1, 3 and 5 days, CCK-8 assays and live/dead cell staining were conducted to detect the viability of cells seeded on the membranes. Briefly, cells were rinsed with PBS for 3 times, and 300 μl of 10 % CCK-8 (Dojindo, CK04, Japan) solution was added and incubated in 37 °C incubators for 90 min. Then 100 μl of the supernatants was transferred into a 96-well plate, and the absorbance of the samples at 450 nm was measured by a Synergy H1 microplate reader (BioTek, USA) (n = 3) [27]. Live/dead cell staining was performed according to the literature [28]. In brief, cells were stained with 2 μmol/L of calcein-AM and 4.5 μmol/L of propidium iodide, and incubated in 37 °C incubators for 90 min. Finally, images were captured by an inverted fluorescence microscope (Nikon, Japan).

Three days later, nuclear and cytoskeletal staining of hPDLSCs and NIH3T3 fibroblasts was carried out to observe the morphology and attachment of the cells seeded on membranes [29]. Cells were fixed with 4 % paraformaldehyde (PFA) for 10 min and rinsed with PBS for 3 times. Next, the cells were permeabilized with 0.5 % Triton X-100 for 5 min and rinsed with PBS for 3 times. Then the cells were incubated with 800 μl of 100 nM phalloidin solution (Yeasen, 40734ES75, China) for 45 min. After that, the cells were stained with 400 μl of 10 μg/mL 2-(4-amidinophenyl)-6-indolecarbamidine dihydrochloride (DAPI) (Beyotime, C1002, China) for 5 min and rinsed with PBS for 3 times. All the procedures were performed at room temperature and protected from the light. Finally, the images were captured by a laser confocal microscope (Nikon, Japan).

2.7. In vitro osteogenic differentiation evaluation

Alkaline phosphatase (ALP) activity, calcium nodules formation and osteogenic genes expression were evaluated to determine the osteogenic differentiation abilities of hPDLSCs on electrospun fibrous membranes. hPDLSCs were seeded on the electrospun fibrous membranes at a density

of 1 × 10^4 cells/well. Seven days later, ALP staining was conducted with a BCIP/NBT alkaline phosphatase color development kit (Beyotime C3206, China). ALP activity in hPDLSCs was measured by an alkaline phosphatase assay kit (Beyotime P0321S, China). 28 days later, ARS staining (Solarbio, G1452, China) was performed to detect the formation of the mineralized nodules. 10 % (w/v) cetylpyridinium chloride (CPC) (Sangon Biotech, A600106-0100, China) solution was added to the stained plates to determine the calcium content of hPDLSCs seeded on the electrospun fibrous membranes, and the absorbance of the extracted dye was detected at 562 nm by a Synergy H1 microplate reader (BioTek, USA) [30]. The stained images were captured by a stereomicroscope (Nikon, Japan).

After hPDLSCs were seeded on the electrospun fibrous membranes for 7 and 14 days, total ribonucleic acid (RNA) of hPDLSCs was extracted by the RNAiso Plus reagent (Takara, 9108, Japan) [31]. A total of 1 μg RNA was reverse transcribed into complementary deoxyribonucleic acid (cDNA) by a PrimeScript RT Master Mix kit (Takara, RR036A, Japan). The expression of ALP, Collagen I (Col-1), osteopontin (OPN), osteocalcin (OCN), vascular endothelial growth factor (VEGF) and hypoxia inducible factor-1α (HIF-1α) was detected by quantitative real-time polymerase chain reaction (qRT-PCR) with a TB Green Premix Ex Taq kit (Takara, RR420A, Japan). The primer sequences are listed in Table S1.

2.8. Immunofluorescence staining of OPN and VEGF

hPDLSCs were seeded on the electrospun fibrous membranes at a density of 1 × 10^4 cells/well. Seven days later, the samples were harvested, and immunofluorescence staining of OPN and VEGF were conducted respectively according to the literature [10]. Cells were fixed with 4 % PFA for 30 min and gently rinsed with PBS for 3 times. Triton X-100 (0.5 %) was employed to penetrate the cells for another 30 min. Then the cells seeded on the electrospun fibrous membranes were blocked with 1 % bovine serum albumin (BSA) for 1 h. Next, the cells were incubated with primary OPN antibody (Proteintech 22952-1-AP, USA, 1:200) and VEGF antibody (Proteintech, 66828-1-Ig, USA, 1:200) respectively at 4 °C overnight. On the second day, the cells were gently rinsed with PBS for 3 times and incubated with Alexa Fluor 488-conjugated goat polyclonal secondary antibody to rabbit IgG (Abcam, ab150077, the UK) for 1 h at room temperature. Finally, the cells were stained with DAPI and phalloidin as previously described. The samples were observed by a laser confocal microscope (Nikon, Japan).

2.9. Cell migration

The migration ability of hPDLSCs on the electrospun fibrous membranes was evaluated by creating a 1 mm width gap with a personalized stainless steel (15 mm diameter with a 1 mm transverse barrier in the middle) as described in the literature [32]. Personalized stainless steels were placed on the electrospun fibrous membranes in a 24-well plate. hPDLSCs were seeded on the membranes at a density of 5 × 10^5 cells/well in 1 mL of α-MEM medium containing 10 % FBS. Twenty-four hours later, personalized stainless steels were removed to create a 1 mm width gap, and the cells were cultured with serum-free medium for another 48 h. Finally, the samples were stained with DAPI and observed by an inverted fluorescence microscope (Nikon, Japan).

2.10. In vitro swelling and degradation of the electrospun fibrous membranes

The e electrospun fibrous membranes were cut into circular shapes (diameter of 34 mm) and immersed in both artificial saliva (Solarbio, A7990, China) and sodium hydroxide solution (pH = 8.5) (Sigma, S8045, USA) to evaluate their swelling and degradation rates. The initial weight of the samples was recorded as M_0. Briefly, the samples were immersed in artificial saliva and sodium hydroxide solution (pH = 8.5) in centrifuge tubes for 2 h and 24 h, respectively, on a 37 °C shaker. After removal from the solution, the membranes were dried with a fine absorbent paper and weighed. The weight of which was recorded as M_d. The swelling rate was calculated using the following equation [23]:

$$\text{Swelling rate}\ (\%) = (M_d - M_0) \ / \ M_0$$

For the degradation rate, the samples were immersed in 20 mL of artificial saliva and sodium hydroxide solution (pH = 8.5) in centrifuge tubes on a 37 °C shaker. The incubation solutions were changed every 2 days. At preset timepoints, the samples were rinsed with deionized water, freeze-dried and weighed, and the weight was recorded as M_t. The degradation rate was calculated using the following equation [33]:

$$\text{Degradation rate}\ (\%) = (M_0 - M_t) \ / \ M_0$$

2.11. In vitro drug release of the electrospun fibrous membranes

The electrospun fibrous membranes were tailored into circular shapes (diameter of 14 mm) and immersed in 10 mL of artificial saliva in a centrifuge tube on a 37 °C shaker. For evaluation of the release of quercetin from the electrospun fibrous membranes, 2 mL of the released solution was collected at preset timepoints. In addition, 2 mL of fresh artificial saliva was added to the centrifuge tube. The absorbance of the collected released solution was measured by an ultraviolet–visible spectrophotometer (UV, 759CRT, China) at a wavelength of 256 nm. The initial weight of the electrospun fibrous membranes was recorded as M_0, $\sum_q$ represented the mass of the cumulatively released quercetin, and c indicated the concentration of quercetin loaded in the electrospun fibrous membranes. The cumulative release of quercetin was calculated using the following equation [23,34].

$$\text{Cumulative drug release rate}\ (\%) = \sum_q \Big/ cM_0$$

2.12. Barrier function of the electrospun fibrous membranes

We evaluated the barrier function of the electrospun fibrous membranes described as the literature [26]. The electrospun fibrous membranes were tailored into circular shapes (diameter of 6 mm), fixed on the cell culture inserts (Falcon, 351,152, USA), and placed in 24-well plates. Human gingival fibroblasts (HGFs) were isolated (Fig. S5) and seeded on the electrospun fibrous membranes for 14 days. The samples were stained with hematoxylin-eosin (HE) and phalloidin. The bottom of the 24-well plate was observed by an optical microscope (Nikon, Japan).

2.13. Animal experiment

Sprague-Dawley (SD) rats (8 weeks old, male, 230–250 g) were purchased from the laboratory animal center of Shanghai Ninth People's Hospital and raised in specific pathogen-free (SPF) conditions. All the animal procedures were approved by the laboratory animal ethics committee of Shanghai Ninth People's Hospital (SH9H-2020-A469-1). Sixteen male 8-week-old SD rats were stochastically divided into 4 groups: (1) the normal group: without periodontal bone defects; (2) the control group: periodontal bone defects without treatment; (3) the PCL group: periodontal bone defects with PCL electrospun fibrous membrane treatment; (4) the 4%Qtn/PCL group: periodontal bone defects with 4% Qtn/PCL electrospun fibrous membrane treatment. Rats were anesthetized with pentobarbital sodium and periodontal bone defects were created as previously described [4]. First, the mucoperiosteal flaps located in the bilateral maxillary first molar were incised, and the palatal alveolar bone contiguous to the root surfaces of the maxillary first molar was removed with a dental drill under saline irrigation. Periodontal bone defects approximately 3 mm (length) x 1.5 mm (width) x 2 mm (depth) were fabricated. Afterward, PCL and 4%Qtn/PCL electrospun fibrous membranes were implanted into the defect sites. Eight

weeks after the surgery, rats were euthanized, and the maxillae of the rats were collected and fixed in 4 % PFA for further detection.

2.14. Microcomputed tomography (micro-CT) assessment

The collected maxillae were scanned by a micro-CT (PerkinElmer, USA) to assess the bone regeneration. Scanning was conducted with a voltage of 90 kV, a current of 90 μA, and a voxel resolution of 72 μm. Caliper Analyze 12.0 software was used to reconstruct and analyze the 3D and 2D images of the alveolar bone. The distance between the enamel-dentinal junction (CEJ) and alveolar bone crest (ABC) was measured to assess the vertical bone loss of the defect sites. In addition, the bone volume/tissue volume (BV/TV) and bone mineral density (BMD) of the defects were quantified.

2.15. Histological staining

All samples were fixed in 4 % PFA at room temperature for 24 h. The samples for hematoxylin and eosin (HE), Masson's trichrome and immunohistochemical staining were decalcified in 10 % ethylenediaminetetraacetie acid (EDTA) (Solarbio, E8030, China) on a shaker at 37 °C for 30 days, dehydrated in different concentrations of ethanol, vitrified in dimethylbenzene, embedded in paraffin and sectioned at a thickness of 5 μm. HE, Masson's trichrome and immunohistochemical staining for OPN and VEGF was conducted according to the literature [35].

2.16. Statistical analysis

All quantitative data are expressed as mean ± standard deviation (SD). Student's *t*-test was used for statistical analysis with SPSS 20.0 software. $*p < 0.05$ was considered statistically significant.

3. Results

3.1. Schematic illustration of the experiment

The fabrication procedure of the electrospun fibrous membranes and their application in periodontal bone regeneration are illustrated in Fig. 1.

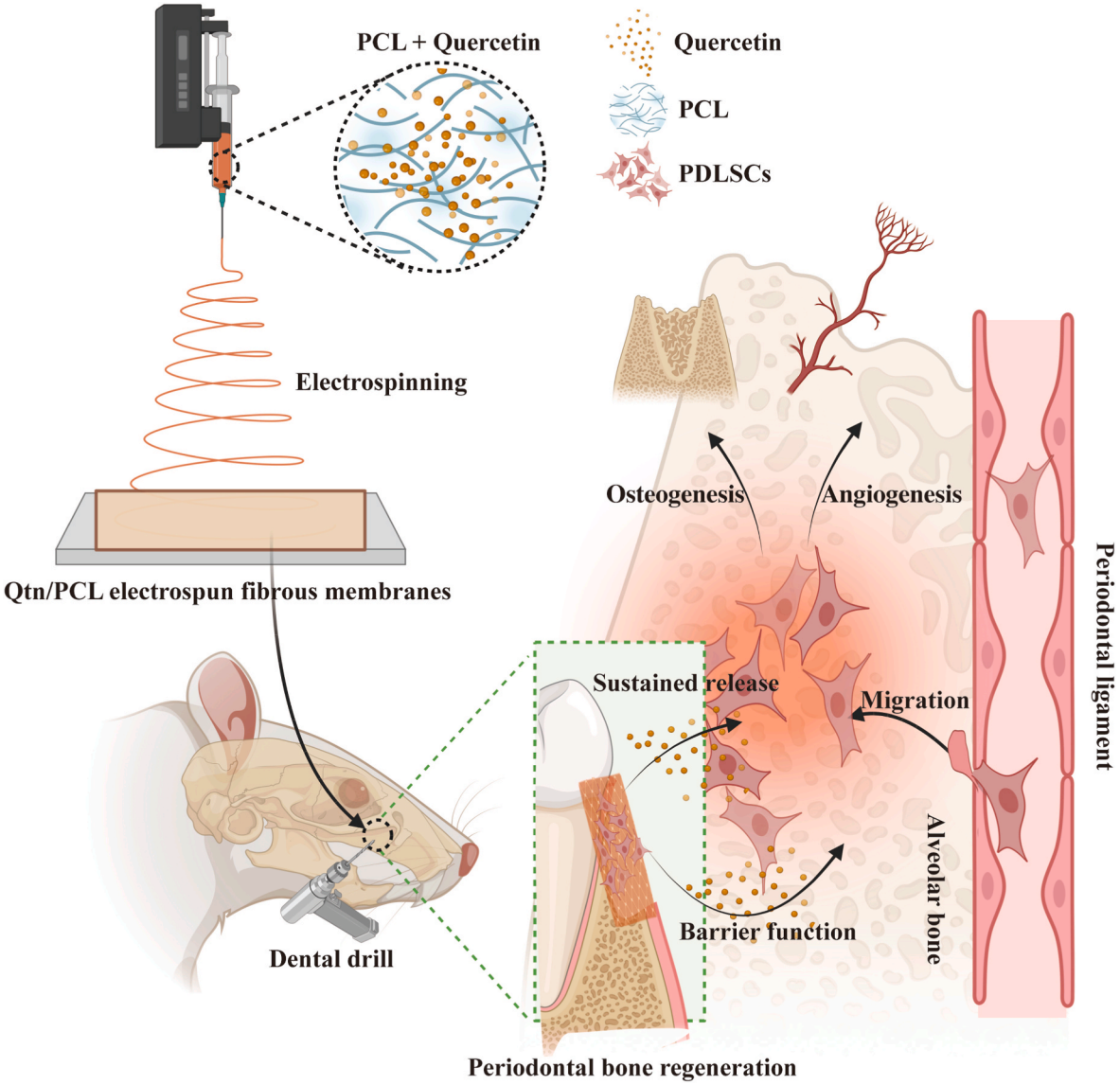

Fig. 1. Fabrication procedure of the electrospun fibrous membranes and their application in periodontal bone regeneration.

3.2. Fabrication and characterization of the electrospun fibrous membranes

All electrospun fibrous membranes, including PCL, 0.5%Qtn/PCL, 1%Qtn/PCL, 2%Qtn/PCL, 4%Qtn/PCL and 8%Qtn/PCL were successfully fabricated and observed by SEM. The SEM results indicated that all fibers were randomly distributed with a smooth appearance, uniform diameter and bead-free morphology (Fig. 2A). The average nanofibers' diameters of each group ranged from 1.76 to 2.14 μm (Fig. 2C, Table 1), which indicated that all membranes were

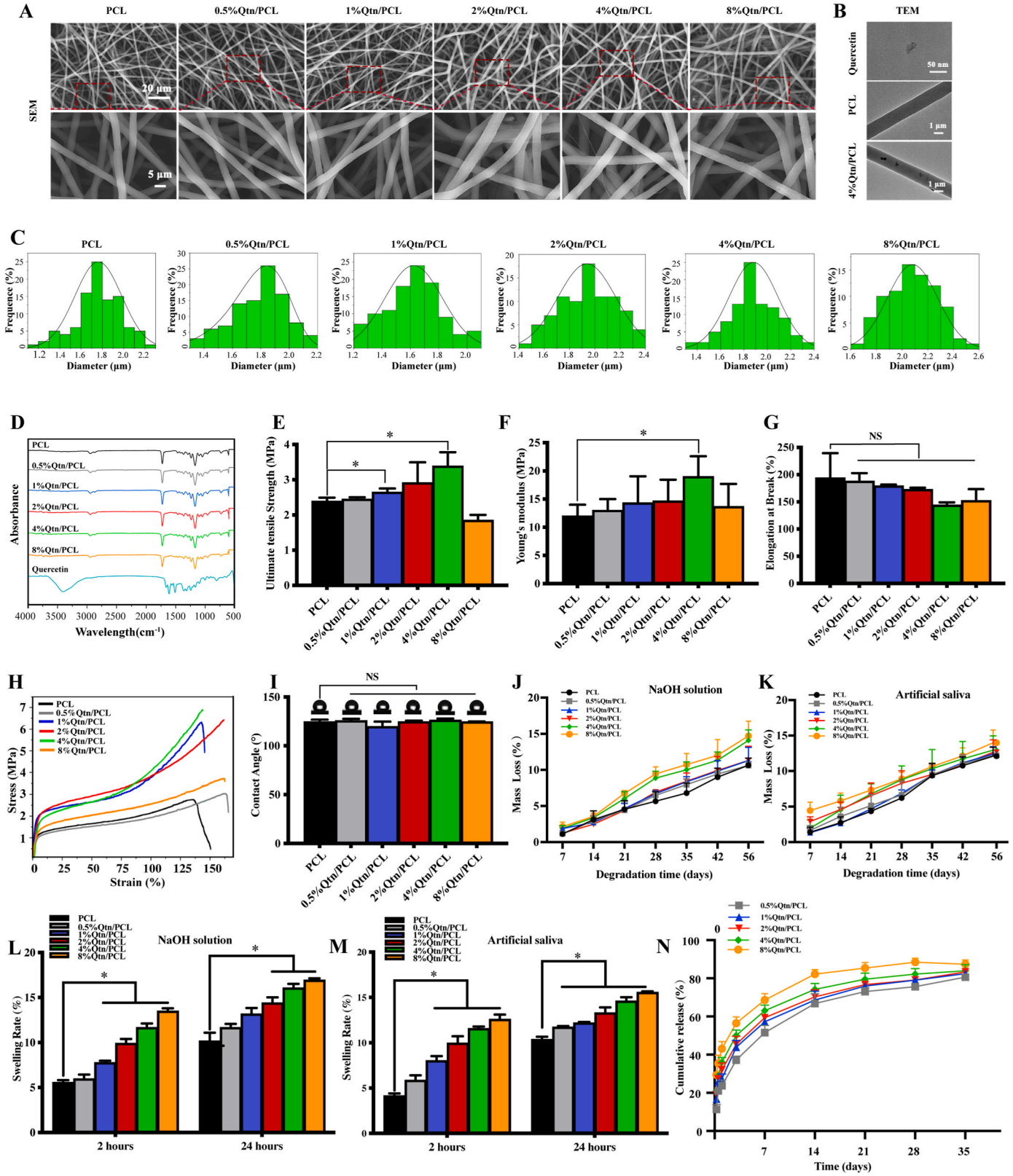

Fig. 2. Characterization of the electrospinning nanofibrous membranes.

Table 1
The average nanofibers' diameters of the electrospun fibrous membranes.

Group	Average diameter of nanofibers (μm)
PCL	1.76 ± 0.22
0.5%Qtn/PCL	1.77 ± 0.21
1%Qtn/PCL	1.79 ± 0.18
2%Qtn/PCL	2.00 ± 0.31
4%Qtn/PCL	1.90 ± 0.22
8%Qtn/PCL	2.14 ± 0.30

micrometer-sized. The incorporation of quercetin into PCL did not alter the morphology of the fibers, and the mean diameters of the fibers were fractionally increased after the incorporation of quercetin. According to the TEM images, quercetin could be observed in the single fiber, which indicated that quercetin was embedded into PCL (Fig. 2B).

ART-FTIR spectra were utilized to analyze the surface chemical properties and characteristic functional groups of the electrospun fibrous membranes (Fig. 2D). The raw PCL material showed characteristic peaks at 2866 and 2944 cm^{-1} attributed to symmetric and asymmetric CH2 stretching, respectively. Characteristic peaks at 1727 and 1172 cm^{-1} due to C═O stretching and C–C stretching, respectively, were also observed. The results are in accordance with previous literature [36]. The ART- FTIR spectra of the 0.5%Qtn/PCL, 1%Qtn/PCL, 2% Qtn/PCL, 4%Qtn/PCL and 8%Qtn/PCL electrospun fibrous membranes resembled those of the raw PCL material, which demonstrated that the surface chemical properties of the Qtn/PCL fibrous membranes were unaffected by the incorporation of quercetin or the electrospinning process.

The mechanical properties of the electrospun fibrous membranes were assessed by a mechanical tester. The ultimate tensile strength, Young's modulus and elongation at break of each group were analyzed (Fig. 2E–G) and presented as mean ± standard deviation (Table 2). The stress-strain curves of the electrospun fibrous membranes were shown in Fig. 2H. With increasing quercetin content, the ultimate tensile strength and Young's modulus of the Qtn/PCL fibrous membranes gradually increased, and the 4%Qtn/PCL fibrous membrane possessed the optimum ultimate tensile strength (3.387 ± 0.395 MPa) and Young's modulus (19.00 ± 3.61 MPa) compared to the ultimate tensile strength (2.393 ± 0.098 MPa) and Young's modulus (12.00 ± 2.00 MPa) of pure PCL group. There were no significant differences in elongation at break between the different groups.

The surface wettability of the electrospun fibrous membranes was assessed by water contact angle analysis. The water contact angles of each group were analyzed (Fig. 2I) and presented as mean ± standard deviation (Table 3). No significant differences were observed among the water contact angles of all the groups.

The degradation and swelling rate of the electrospun fibrous membranes were detected in both NaOH solution (pH = 8.5) and artificial saliva. The results indicated that the mass loss of the electrospun fibrous membranes within 14 days was no more than 6 %. Electrospun fibrous membranes incorporated with quercetin showed a faster mass loss compared with the PCL group (Fig. 2J and K). Along with the degradation and release of quercetin, damaged polymer fibers might interact with the solution. The swelling rate was evaluated after the electrospun fibrous membranes were immersed in NaOH solution (pH = 8.5) and artificial saliva for 2 h and 24 h, respectively. A higher uptake rate in aqueous solution was observed in Qtn/PCL membranes (Fig. 2L-M), which was in accordance with the degradation profile of the electrospun fibrous membranes.

The *in vitro* quercetin release of the Qtn/PCL fibrous membranes was also detected. Our results suggested that the Qtn/PCL fibrous membranes exhibited a sustained and long-term release profile (Fig. 2N). The cumulative release rates were relatively fast within 14 days, and reached over 80 % at 35 days.

Table 2
Mechanical properties of the electrospun fibrous membranes.

Group	Ultimate tensile strength (MPa)	Young's modulus (MPa)	Elongation at break (%)
PCL	2.393 ± 0.098	12.00 ± 2.00	194 ± 45.57
0.5%Qtn/PCL	2.450 ± 0.050	13.00 ± 2.00	188 ± 14.73
1%Qtn/PCL	2.650 ± 0.100	14.33 ± 4.73	179 ± 2.52
2%Qtn/PCL	2.917 ± 0.577	14.67 ± 3.79	173 ± 3.22
4%Qtn/PCL	3.387 ± 0.395	19.00 ± 3.61	144 ± 5.00
8%Qtn/PCL	1.850 ± 0.150	13.67 ± 4.04	152 ± 21.13

Table 3
The water contact angles of the electrospun fibrous membranes.

Group	Water contact angle (°)
PCL	124.8 ± 2.02
0.5%Qtn/PCL	125.8 ± 1.89
1%Qtn/PCL	119.8 ± 4.93
2%Qtn/PCL	124.8 ± 1.04
4%Qtn/PCL	126.3 ± 1.61
8%Qtn/PCL	124.7 ± 0.29

A. SEM images of the electrospun fibrous membranes. B. TEM images of quercetin powder and the electrospun fibrous membranes. C. Diameter distribution of the electrospun fibrous membranes. D. ART-FTIR spectra of the electrospun fibrous membranes. E. Ultimate tensile strength. F. Young's modulus. G. Elongation at break. H. Stress-strain curve. I. Water contact angle analysis. J-K. Degradation rate of the electrospun membranes in sodium hydroxide solution and artificial saliva respectively. L-M. Swelling rate of the electrospun membranes in sodium hydroxide solution and artificial saliva respectively. N. Cumulative release of quercetin in artificial saliva from the electrospun fibrous membranes. $P^* < 0.05$ versus PCL group.

3.3. Cytocompatibility of the electrospun fibrous membranes

Both hPDLSCs and NIH3T3 fibroblasts were seeded on the electrospun fibrous membranes respectively. Then cell viability was assessed by CCK-8 assays and live/dead cell staining, and cell morphology and adhesion were assessed by cytoskeletal staining.

The CCK-8 assay was conducted after cell seeding for 1, 3 and 5 days. The results suggested that the viabilities of hPDLSCs seeded on the 4% Qtn/PCL and 8%Qtn/PCL electrospun fibrous membranes were promoted compared to those seeded on the PCL electrospun fibrous membranes on Day 3 and Day 5. In addition, the viability of hPDLSCs seeded on the 2%Qtn/PCL electrospun fibrous membranes on Day 5 was also promoted (Fig. 3A). For NIH3T3 fibroblasts, the viabilities of cells seeded on the 1%Qtn/PCL, 2%Qtn/PCL, 4%Qtn/PCL and 8%Qtn/PCL electrospun fibrous membranes for 5 days were significantly increased (Fig. 3B).

Live/dead cell staining was carried out after cell seeding for 3 days. According to the live/dead cell staining results, both hPDLSCs and NIH3T3 fibroblasts grew very well on the electrospun fibrous membranes (Fig. 3C). There were barely any dead cells (red fluorescence) in the fields, and the majority of the cells were stained green fluorescence, which demonstrated that the electrospun fibrous membranes had no cytotoxic effects on the two kinds of cells. Moreover, a higher intensity of green fluorescence in hPDLSCs was observed in 4%Qtn/PCL and 8% Qtn/PCL fibrous membranes, which is in accordance with the CCK-8 results in Fig. 3A (Fig. S3C).

Cytoskeletal staining was performed 3 days after cells were seeded on the electrospun fibrous membranes. F-actin in the cytoskeleton was stained with phalloidin, which is represented as red fluorescence, and

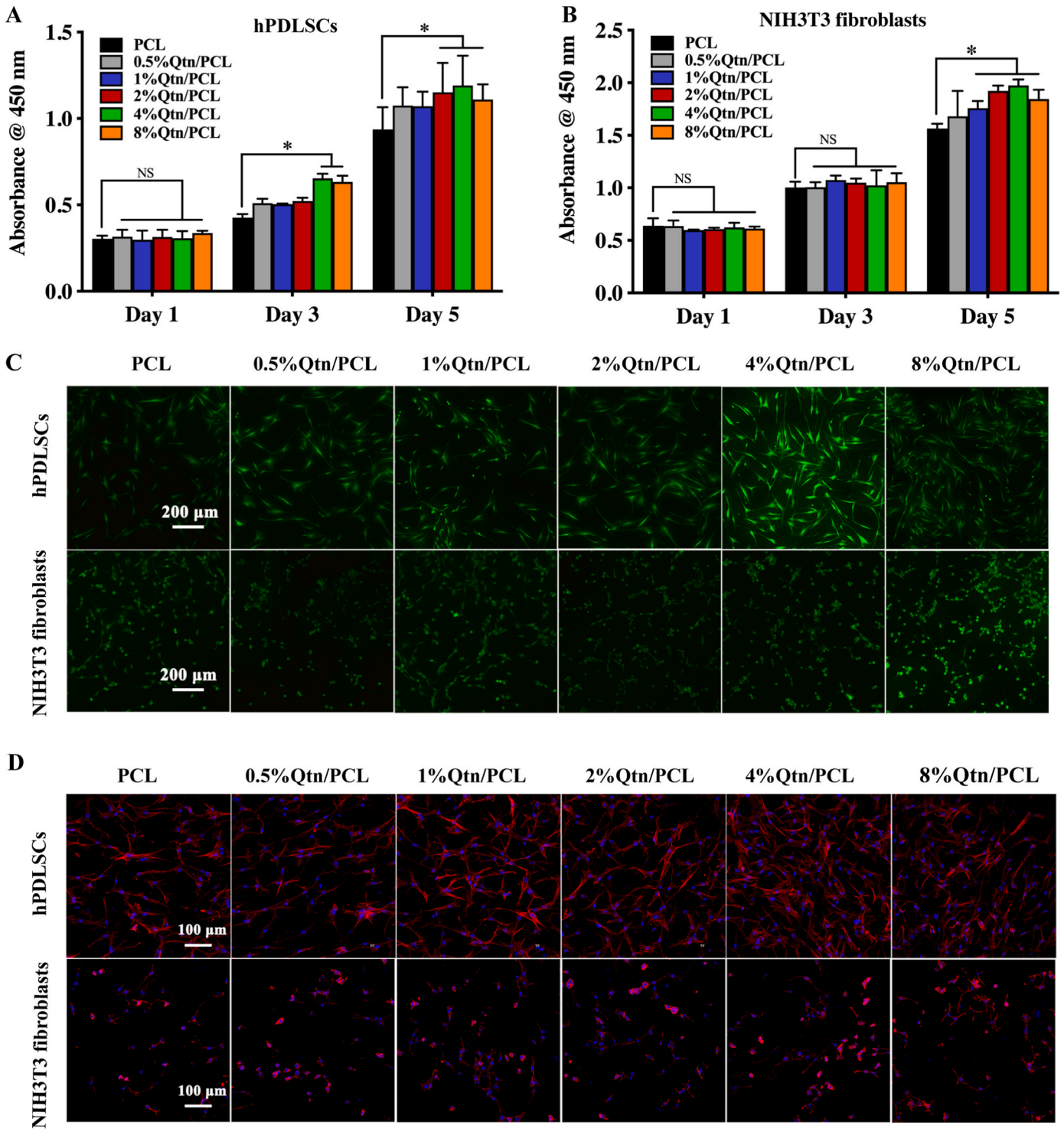

Fig. 3. Cytocompatibility evaluation of the electrospun fibrous membranes.

nuclei were stained with DAPI, which is represented as blue fluorescence. Both hPDLSCs and NIH3T3 fibroblasts were evenly distributed and well attached to the electrospun fibrous membranes. NIH3T3 fibroblasts on the electrospun fibrous membranes showed relatively round shapes, while hPDLSCs appeared to have a flattened morphology with elongated filopodia (Fig. 3D).

Taken together, the Qtn/PCL electrospun membranes exhibited good cytocompatibility and did not show negative effects on the proliferation, adhesion or cellular morphology to both hPDLSCs and NIH3T3 fibroblasts.

A-B. Cell viability was detected by CCK-8 assays after hPDLSCs and NIH3T3 fibroblasts were cultured on the electrospun fibrous membranes for 1, 3 and 5 d respectively. C. Live/dead cell staining was performed after hPDLSCs and NIH3T3 fibroblasts were cultured on the electrospun fibrous membranes for 3 d respectively. D. F-actin and nuclei staining of hPDLSCs and NIH3T3 fibroblasts cultured on the electrospun fibrous membranes for 3 d respectively. $P^* < 0.05$ versus PCL group.

3.4. Osteogenic/angiogenic differentiation of hPDLSCs induced by Qtn/PCL fibrous membranes

The osteogenic and angiogenic effects of the electrospun fibrous membranes on hPDLSCs were explored by ALP staining, ALP activity quantification, ARS staining, mineralized calcium nodule quantification, cellular immunofluorescence staining and RT-qPCR. As indicated by ALP staining, hPDLSCs had higher ALP activity on the 2%Qtn/PCL and 4%Qtn/PCL electrospun fibrous membranes than on the pure PCL membrane at both 7 and 14 d (Fig. 4A). Quantitative evaluation of ALP activity suggested that 1%Qtn/PCL, 2%Qtn/PCL and 4%Qtn/PCL electrospun fibrous membranes considerably enhanced the ALP activity of hPDLSCs at 7 and 14 d compared with the pure PCL membranes, which was in accordance with the ALP staining results. In addition, the general ALP activity of hPDLSCs at 14 d was remarkably elevated compared with that at 7 d (Fig. 4C). ARS staining and quantification were performed to detect the formation of the mineralized calcium nodules of hPDLSCs at 28 d. The results showed that the amount of the mineralized calcium nodules of hPDLSCs on the Qtn/PCL electrospun fibrous membranes slightly increased, which indicated that the incorporation of quercetin promoted the calcium deposition of hPDLSCs (Fig. 4B and D).

Immunofluorescence staining of OPN and VEGF was performed after hPDLSCs were cultured on the electrospun fibrous membranes for 7 d. Representative images showed that hPDLSCs cultured on 2%Qtn/PCL and 4%Qtn/PCL electrospun fibrous membranes exhibited higher OPN protein levels (Fig. 4E). Besides, hPDLSCs cultured on 2%Qtn/PCL group exhibited higher VEGF protein level (Fig. 4F).

hPDLSCs were cultured on the electrospun fibrous membranes for 7 or 14 d, and RT-qPCR was conducted to analyze the expression of osteogenic- and angiogenic-related genes in hPDLSCs. The gene expression of ALP in the 2%Qtn/PCL and 4%Qtn/PCL group was remarkably higher than that in the PCL group (Fig. 4G). Similarly, the gene expression of Col-1 in the 2%Qtn/PCL, 4%Qtn/PCL and 8%Qtn/PCL group was dramatically higher than that in the PCL group (Fig. 4H). The results indicated that the gene expression of OPN and OCN was significantly higher in the 1%Qtn/PCL, 2%Qtn/PCL, 4%Qtn/PCL and 8%Qtn/PCL group than in the PCL group. Additionally, the expression of the OCN gene was also increased in the 0.5%Qtn/PCL group compared with the PCL group (Fig. 4I and J). Moreover, we examined the expression of angiogenic-related genes, including VEGF and HIF-1α, after cells were seeded on the membranes for 7 d. The results suggested that the gene expression of VEGF was significantly higher in the 0.5% Qtn/PCL,1%Qtn/PCL, 2%Qtn/PCL and 4%Qtn/PCL groups than in the PCL group (Fig. 4K). The gene expression of HIF-1α was significantly higher in the 0.5%Qtn/PCL,1%Qtn/PCL and 2%Qtn/PCL groups than in the PCL group (Fig. 4L).

Taken together, all these results demonstrated that the incorporation of quercetin into PCL electrospun fibrous membranes promoted the osteogenic and angiogenic differentiation processes. The controlled release of quercetin from the electrospun fibrous membranes significantly enhanced the osteogenic and angiogenic differentiation of hPDLSCs. Furthermore, the 4 % Qtn/PCL electrospun fibrous membrane exhibited better abilities to induce the osteogenic and angiogenic differentiation of hPDLSCs than the other membranes.

A. ALP staining was performed after hPDLSCs seeded on the electrospun fibrous membranes for 7 and 14 d respectively. B. ARS staining was performed after hPDLSCs seeded on the electrospun fibrous membranes for 28 d. C. ALP activities of hPDLSCs were detected after cultured on the electrospun fibrous membranes for 7 and 14 d respectively. D. Quantification of mineral nodules of hPDLSCs after seeded on the electrospun fibrous membranes for 28 d. E-F. Immunofluorescence staining of OPN and VEGF were performed respectively after hPDLSCs cultured on the electrospun fibrous membranes for 7 d. G-J. The expression of ALP, Col-1, OPN and OCN mRNA were detected by RT-qPCR respectively after hPDLSCs cultured on the electrospun fibrous membranes for 7 d or 14 d. K–I. The expression of VEGF and Hif-1α mRNA were detected by RT-qPCR respectively after hPDLSCs cultured on the electrospun fibrous membranes for 7 d. P*< 0.05 versus PCL group.

3.5. Effects of the electrospun fibrous membranes on the migration of hPDLSCs

The concrete procedures of the cellular migration assay are illustrated in Fig. 5B. Briefly, the electrospun fibrous membranes were placed in the bottom of 24-well plates, and personalized stainless steels were placed on the membranes. After cells were seeded on the electrospun fibrous membranes for 24 h, the stainless steels were removed, and 1 mm wide artificial gaps were created. Then the culture medium of hPDLSCs was replaced with serum-free medium which containing 1 % penicillin-streptomycin. Forty-eight hours later, cells seeded on the electrospun fibrous membranes were fixed in 4 % PFA, and nuclei were stained with DAPI. Representative images of cell migration and quantitative analysis results suggested that the migration rates of hPDLSCs on the 1%Qtn/PCL, 2%Qtn/PCL, 4%Qtn/PCL and 8%Qtn/PCL electrospun fibrous membranes were remarkably higher than those on the PCL membranes (Fig. 5A and C). The results indicated that the incorporation of quercetin into PCL increased the migration of hPDLSCs on the electrospun fibrous membranes.

A. Nuclei fluorescence staining of hPDLSCs after activating cell migration for 0 and 48 h. B. Sketch map of the migration of hPDLSCs on the electrospun fibrous membranes. C. Statistical analysis of the migration rate of hPDLSCs on the electrospun fibrous membranes. *P**< 0.05 versus PCL group.

3.6. The barrier function of the electrospun fibrous membranes

In this study, we set up a transwell model to detect the anti-cellular penetration capacity of the membranes (Fig. 6A). HE staining results showed that HGFs did not penetrate the membranes (Fig. 6B). In addition, images of the lower chamber of the transwell plate were obtained by a light microscope, and no fibroblasts were observed in the lower chamber of the transwell plate (Fig. 6B). Similar results can be found in confocal layer scanning (Fig. 6C).

All these results indicated that the electrospun fibrous membranes possessed an anti-cellular penetration capacity and could exert a barrier function in GTR.

A. Sketch map of the barrier function of the electrospun fibrous membranes. B. HGFs were seeded on the fibrous membranes for 14 d. HE staining were performed on the cross section of the cell-seeded membranes. Images of the lower chamber were captured by a light microscope. C. Top and side views of the cytoskeleton on the membranes were captured by a laser confocal microscope.

3.7. In vivo evaluation of the Qtn/PCL electrospun fibrous membranes on rat periodontal regeneration

To further evaluate the *in vivo* effects of the Qtn/PCL fibrous membranes on periodontal bone regeneration, we established rat periodontal bone defect models, and Qtn/PCL fibrous membranes were transplanted into the periodontal bone defect sites. All the animals were raised in SPF conditions for 8 weeks with no evidence of infection after surgery.

Representative 3D-reconstructed and 2D-sectioned images of micro-CT revealed the bone volume in periodontal defect sites. As 3D reconstruction indicated, there was a significant bone defect in the palatal alveolar bone of the maxillary first molar in the control group. Considerable new bone formation was observed in the periodontal defect sites treated with the membranes compared with that of the control group, especially in the 4%Qtn/PCL group (Fig. 7A). In addition, the distance between the cemento-enamel junction (CEJ) and alveolar bone crest (ABC) markedly increased in the control group compared with the normal group, which demonstrated that there was a significant vertical

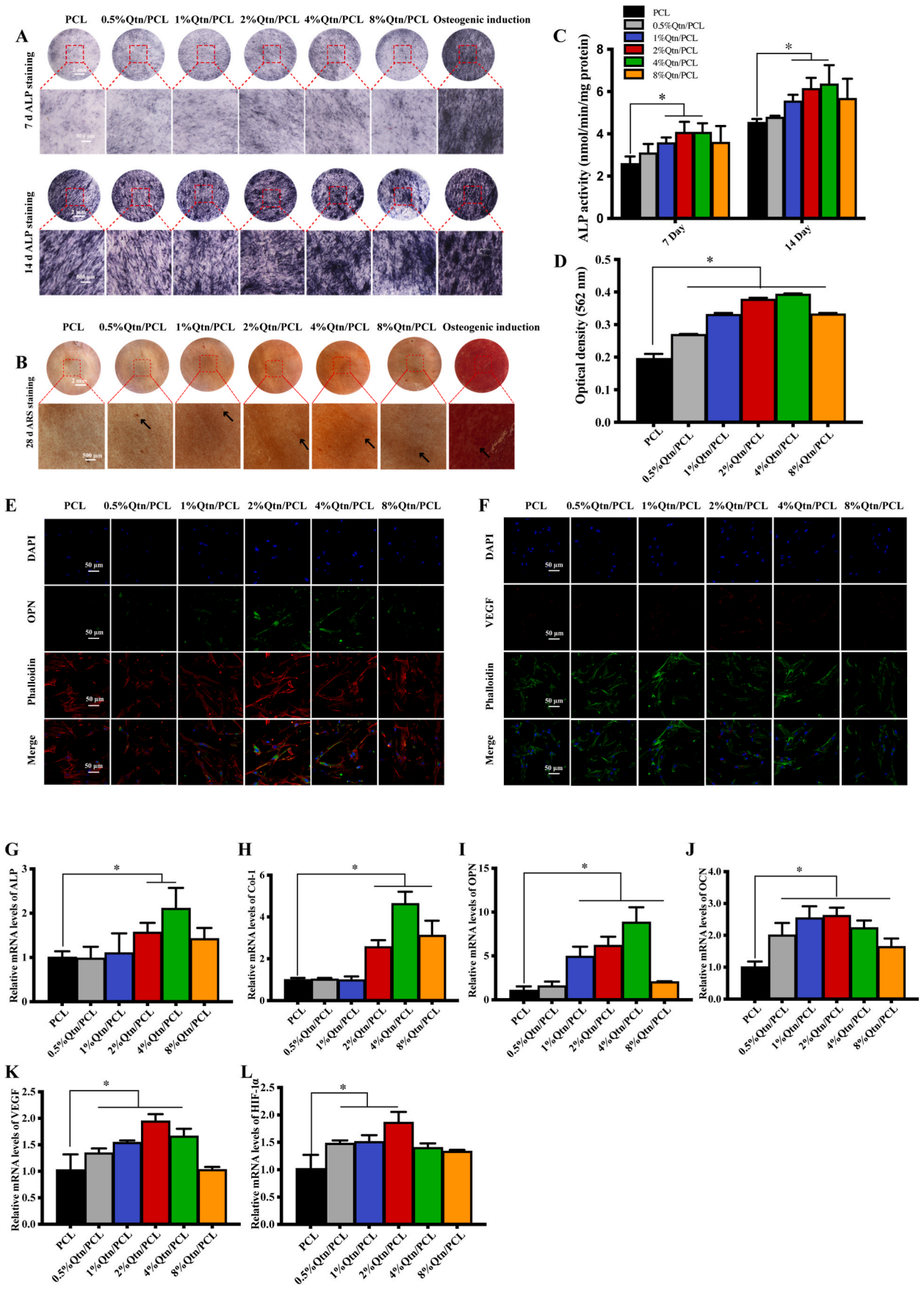

Fig. 4. Osteogenic/angiogenic differentiation of hPDLSCs induced by Qtn/PCL fibrous membranes.

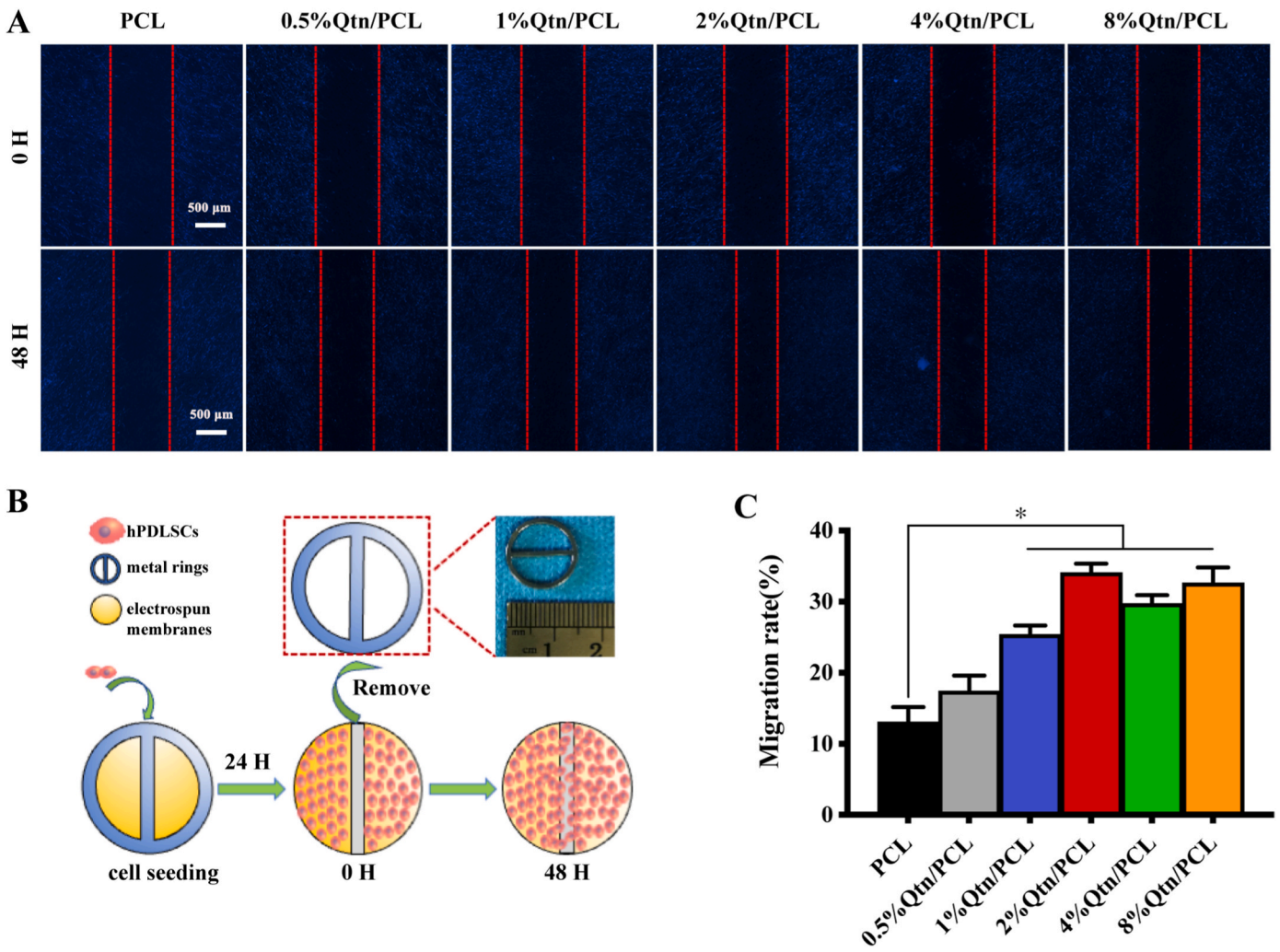

Fig. 5. Effects of the electrospun fibrous membranes on the migration of hPDLSCs.

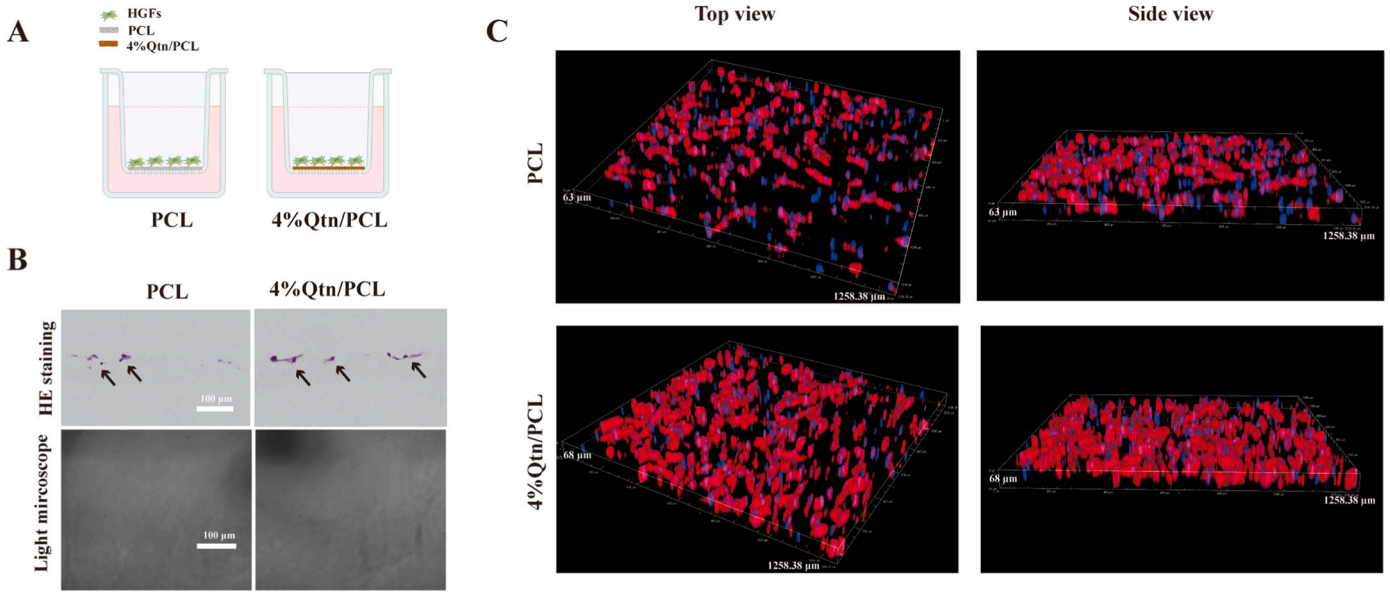

Fig. 6. The barrier function of the electrospun fibrous membranes.

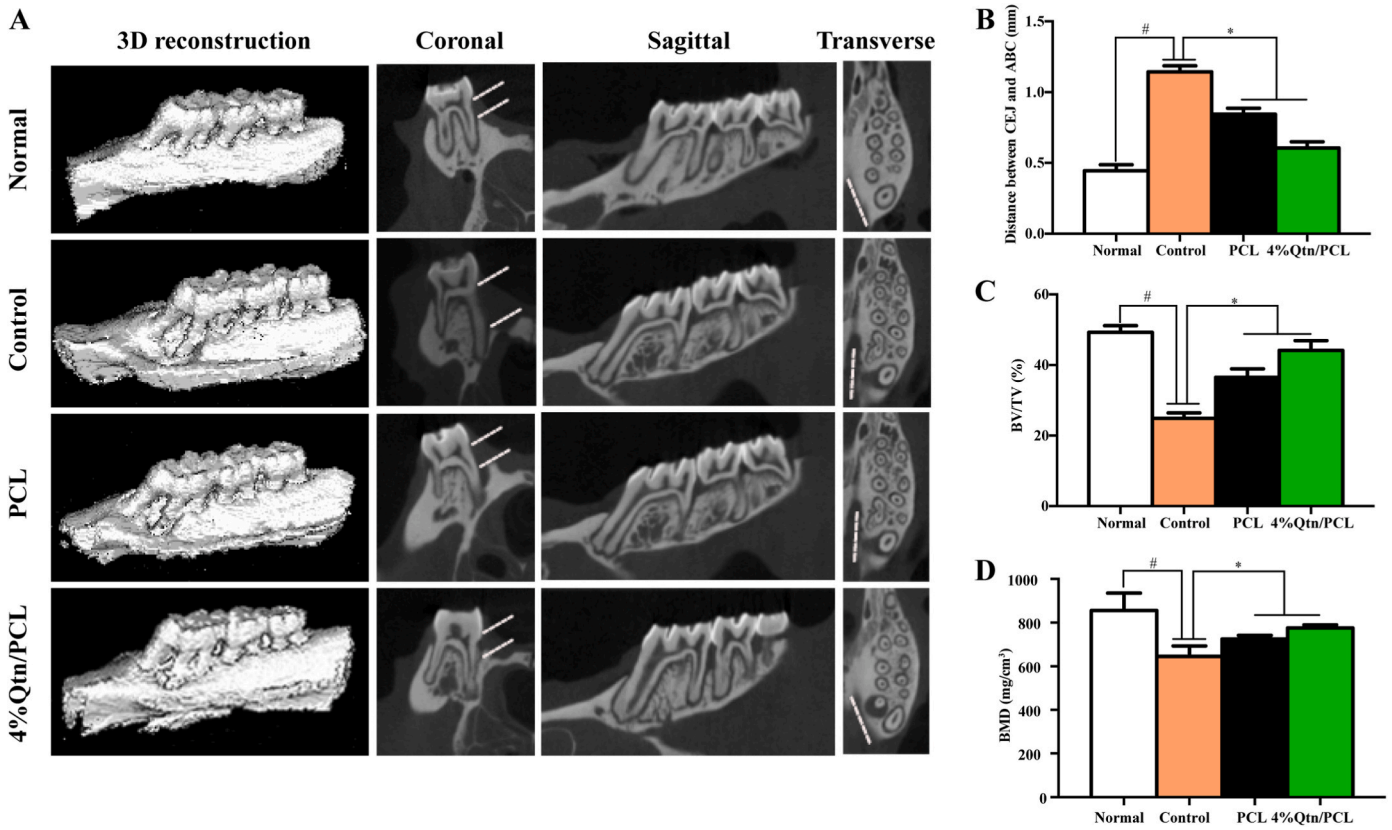

Fig. 7. Radiographic evaluation of the electrospun fibrous membranes in rat periodontal bone regeneration.

bone loss in the rats of the control group. However, a decreased distance between the CEJ and ABC was observed in the 4%Qtn/PCL group, indicating that there was a vertical bone gain (Fig. 7B). The ratio of bone volume (BV) to the total volume (TV) is often regarded as an indicator of the amount of regenerated alveolar bone. The results showed that the levels of BV/TV and BMD in the control group significantly decreased compared with the those in the normal group but gradually increased in the groups transplanted with electrospun fibrous membranes, especially in the 4%Qtn/PCL group (Fig. 7C and D).

HE and Masson's staining indicated that normal alveolar bone appeared wedge-shaped, and was surrounded radially by the periodontal ligament. In control group, only very few new bone formed, and the bone defect site was filled with plenty of connective tissues. There were some new formed segmental bone growing surrounded the PCL electrospun fibrous membranes, and the other part of the defect was colonized with connective tissues. In 4%Qtn/PCL group, new formed segmental bone surrounded the PCL electrospun fibrous membranes and deposited on the defected alveolar bone were observed, while the alveolar ridge was still relatively low and flat (Fig. 8A and B). The expression of OPN and VEGF in new bone formation area were detected by immunohistochemical staining. The expression of OPN and VEGF positive cells in new bone formation area was slightly higher in the Qtn/PCL group than other groups (Fig. 8C–D, Fig. S4).

A. Three-dimensional reconstruction and sectioned views of the rat maxillary alveolar bone. B. The distance between cemento-enamel junction and alveolar bone crest. C. Bone volume/total volume. D. Bone mineral density. $P^{*} < 0.05$ versus control group, $P^{\#} < 0.05$ versus normal group.

A. Representative images of HE staining. B. Representative images of Masson's staining. C. Representative images of OPN immunohistochemical staining. D. Representative images of VEGF immunohistochemical staining. AB: alveolar bone, PDL: periodontal ligament, DE: detin, NAB: newly alveolar bone. Red arrows represent OPN or VEGF positive cells.

4. Discussion

Electrospinning is a versatile and cost-effective procedure to fabricate fibrous membranes with the fibers' diameters ranged from nanometers to micrometers. The electrospun fibrous membranes possess a relatively high surface area to volume ratio that endow them with effective drug loading and encapsulation efficacies [37]. In this study, we incorporated quercetin into PCL to fabricate the Qtn/PCL electrospun fibrous membranes via electrospinning. First, we characterized the fabricated electrospun fibrous membranes including the physicochemical and mechanical properties. Then, the effects of the Qtn/PCL fibrous membranes on osteogenesis and angiogenesis were evaluated both *in vitro* and *in vivo*. The cytocompatibility, barrier function and the effects of the Qtn/PCL fibrous membranes on cell migration were also evaluated.

Surface morphology of the electrospun fibrous membranes has pivotal impacts on cellular behaviors, such as cellular adhesion, proliferation and migration [38]. The fabricated membranes exhibited a smooth appearance, and the fibers were uniform and bead-free (Fig. 2A and B). The diameters of the Qtn/PCL membranes slightly increased owing to the incorporation of quercetin into the fibers (Fig. 2C, Table 1). The ATR-FTIR spectra revealed that the spectra of Qtn/PCL fibrous membranes were similar to the spectrum of the raw PCL (Fig. 2D). The results suggested that the incorporation of quercetin and the electrospinning process didn't influence the surface chemical properties of the electrospun membranes. There were no typical peaks of quercetin were observed in the spectra of Qtn/PCL fibrous membranes which indicated that quercetin was incorporated in the interior of the fibers. Topographical structural alterations of biomaterials can be recognized by filipodia on cellular membranes and triggered a series of cellular regulation [39]. The unaltered surface morphology can arrest this situation.

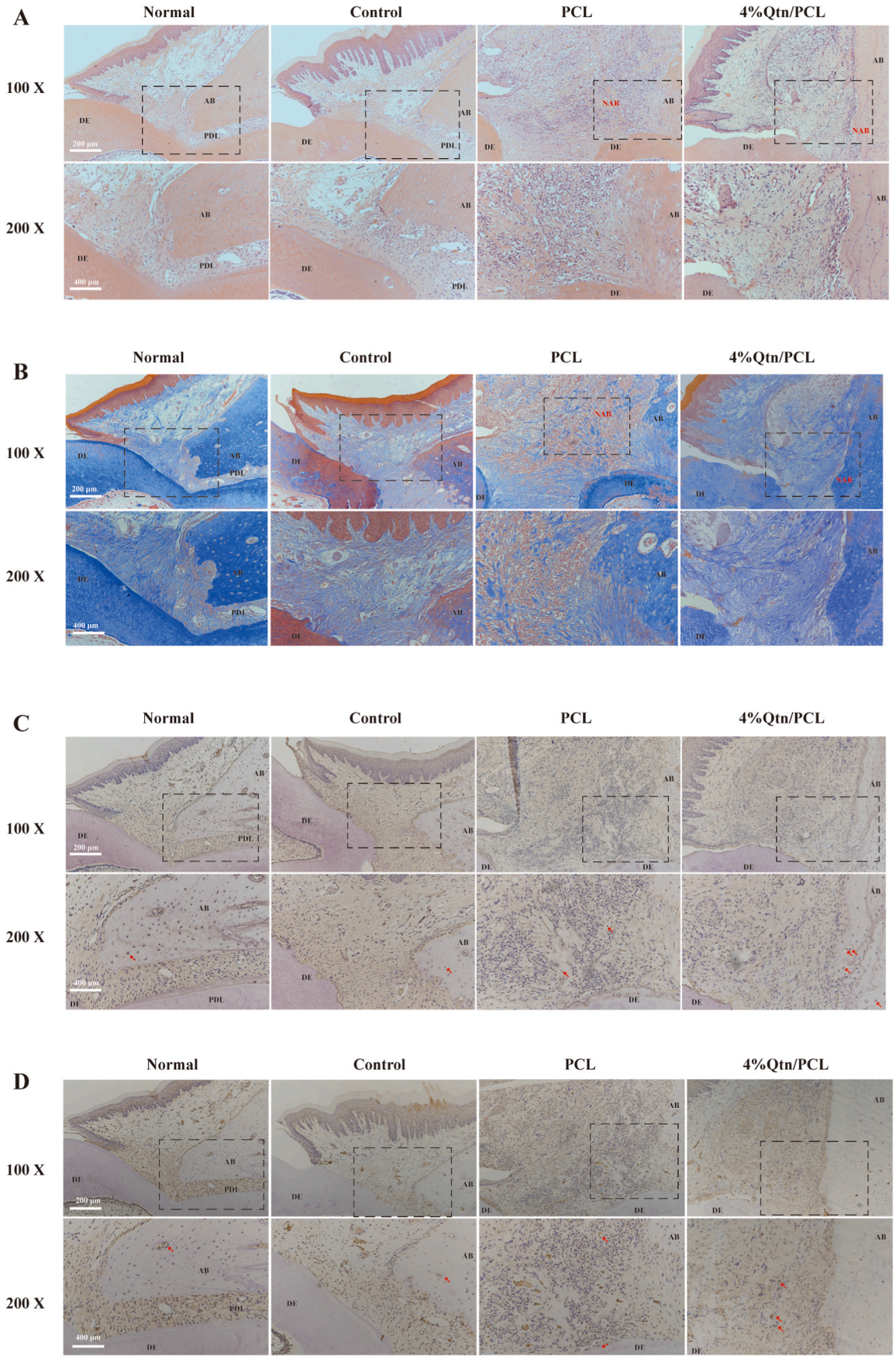

Fig. 8. Histological evaluation of the rat periodontal bone.

GTR membranes for periodontal bone regeneration need possess enough mechanical strength to resist both external forces originated from oral activities and internal force originated from tissue regeneration [18]. Our results suggested that the incorporation of quercetin slightly increased the ultimate tensile strength and Young's modulus of the membranes (Fig. 2E–H). We considered the incorporation of quercetin into PCL fibers reinforced the mechanical strength of the membranes to some extent.

PCL was considered as hydrophobic biomaterials. The contact angels of the electrospun fibrous membranes were greater than 90° and showed hydrophobic features (Fig. 2I, Table 3), which was in accordance with previous literature [40]. The incorporation of quercetin did not improve the wettability of the Qtn/PCL membranes. It may be ascribed to the poor hydrophilic property of quercetin [41]. However, there were no significant differences between the water contact angles of the PCL and the Qtn/PCL membranes. The hydrophobic feature of PCL has negative effects on cell adhesion and proliferation, which may further cytocompatibility of the materials [42]. Otherwise, the incorporation of quercetin could improve this situation via promoting cell proliferation (Fig. 3A and B).

During the wound healing process, the microenvironment of the tissue changes from neutral to slightly alkaline. Thus, we evaluated the degradation and swelling rate in both artificial saliva (pH = 7.4) and NaOH solution (pH = 8.5) in 37 °C to mimic the wound healing process in oral cavity [4]. Membranes for periodontal bone regeneration should keep a suitable degradation rate *in vivo*. A faster degradation rate may result in the gingival soft tissues growing into the defect sites. The membranes may remain in the new formed bone with a slow degradation rate [43]. Our results suggested that within the first 2 weeks, the mass loss of the electrospun fibrous membranes was no more than 6 % in artificial saliva and NaOH solution. The degradation rate reached approximately 15 % at 8 weeks. Electrospun fibrous membranes containing high concentrations of quercetin presented a relatively higher degradation rate (Fig. 2J and K). The Qtn/PCL membranes showed a higher aqueous solution uptake (Fig. L–M), which was in accordance with the degradation file of the membranes. Cumulative release results suggested that the Qtn/PCL membranes release over 50 % of quercetin in 7 days, and reached approximately 80 % in 35 days, exhibiting a sustained release profile (Fig. 2N).

GTR membranes for periodontal regeneration need to have good cytocompatibility to both the soft and hard tissues. Therefore, we evaluated the cytocompatibility of the electrospun fibrous membranes to both PDLSCs and NIH3T3 fibroblasts. Our results indicated that the Qtn/PCL electrospun fibrous membranes showed no cytotoxicity on hPDLSCs and NIH3T3 fibroblasts. Besides, the proliferation of hPDLSCs on day 3 and day 5 was promoted. The proliferation of NIH3T3 fibroblasts seeded on the electrospun fibrous membranes also increased (Fig. 3A–C). The release of quercetin into the culture medium stimulated the proliferation of quercetin, which was in accordance with the previous literature [14,44]. Both hPDLSCs and NIH3T3 fibroblasts were evenly distributed and well attached to the electrospun fibrous membranes (Fig. 3D).

Cell migration plays a pivotal role in many physiological processes, such as morphogenesis, metastatic growth, tissue repair and wound healing [45]. In this research, we created a 1 mm wide artificial gap with a personalized stainless steel to evaluate the migration of hPDLSCs on the electrospun fibrous membranes. The results indicated that the migration of hPDLSCs on the Qtn/PCL membranes was slightly promoted compared with the PCL membranes (Fig. 5). We consider this might attributed to the release of quercetin into the culture medium, but the potential mechanisms need to be further verified. The fundamental function of the GTR membranes is act as a barrier between the gingiva and the alveolar bone, preventing the gingival epithelial and connective tissues from growing into the defect site during the process of periodontal regeneration [46].

The ideal membranes for GTR should possess a barrier function that can prevent soft tissues from growing into bone defect sites, thus creating enough space for new bone formation. GTR membranes for periodontal regeneration must possess the properties that can prevent gingival epithelial and connective tissues from growing into the defect site. The majority of cells in human gingiva is HGFs. In our study, HGFs could not penetrate the electrospun fibrous membranes, creating a stable space for periodontal bone regeneration (Fig. 6).

The ALP and Col-1 genes are involved in the early stage of osteogenic differentiation of stem cells, OPN and OCN are critical genes that participate in the late stage of osteogenic differentiation of stem cells [47]. ALP staining and quantification results suggested that the Qtn/PCL fibrous membranes significantly increased the expression of ALP (Fig. 4A and C). The same result could be observed in ARS staining and quantification assay. There were mineralized calcium nodules deposited on the Qtn/PCL fibrous membranes (Fig. 4B and D). The expression of osteogenic-related genes such as ALP, Col-1, OPN and OCN of hPDLSCs was also increased in the Qtn/PCL fibrous membranes (Fig. 4G–J). These results indicated that the Qtn/PCL fibrous membranes promoted the osteogenic differentiation of hPDLSCs in both early and later stages of osteogenesis. The expression of angiogenic-related genes including VEGF and HIF-1α was elevated in hPDLSCs seeded on the Qtn/PCL electrospun fibrous membranes (Fig. 4K-L). hPDLSCs seeded on the Qtn/PCL electrospun fibrous membranes expressed more VEGF protein as indicated by the immunofluorescence staining (Fig. 4D). Our *in vivo* results revealed that new bone formation was observed in the periodontal defect sites in the 4%Qtn/PCL electrospun fibrous membranes (Fig. 7). The immunohistochemical staining results suggested that the expression of OPN and VEGF positive cells in new bone formation area was slightly higher in 4%Qtn/PCL group (Fig. 8), which was in accordance with the *in vitro* results. Studies reported that quercetin promoted osteogenic differentiation of mouse BMSCs by activating the AMPK/-SIRT1 signaling pathway [48]. As a naturally existed polyphenol, quercetin plays an important role in promoting the osteogenic and angiogenic differentiation of bone marrow-derived mesenchymal stem cells (BMSCs) and adipose-derived mesenchymal stem cells (ADSCs) as previously reported [13,44]. Our previous study revealed that the osteogenesis and angiogenesis of ovariectomized rat BMSCs were reinforced by quercetin [14]. We consider the sustained release of quercetin from the Qtn/PCL electrospun fibrous membranes promoted the osteogenic and angiogenic differentiation of hPDLSCs. But the potential mechanisms need to be further verified.

5. Conclusion

In conclusion, we successfully constructed a multifunctional Qtn/PCL fibrous membrane that enhanced the osteogenic and angiogenic differentiation of hPDLSCs *in vitro* and promoted rat periodontal bone regeneration *in vivo*. The incorporation of quercetin into the fibrous membranes endowed them with reinforced mechanical properties, including ultimate tensile strength and Young's modulus, sustained release of quercetin and a tunable degradation profile. The Qtn/PCL fibrous membranes possessed good cytocompatibility, and both hPDLSCs and NIH3T3 fibroblasts grew and adhered well on the Qtn/PCL fibrous membranes. In particular, the Qtn/PCL fibrous membranes markedly enhanced the osteogenic and angiogenic differentiation and migration of hPDLSCs compared to PCL membranes. In addition, the Qtn/PCL fibrous membranes exerted a barrier function by preventing HGFs from growing into periodontal bone defect sites. Our *in vivo* study proved that 4%Qtn/PCL electrospun fibrous membranes exhibited a better periodontal bone regeneration impact. Taken together, our results demonstrated that the electrospun fibrous Qtn/PCL membranes might be a new strategy for periodontal bone regeneration.

CRediT authorship contribution statement

Yue Hu: Conceptualization, Data curation, Formal analysis,

Investigation, Methodology, Writing - original draft, Writing - review & editing. **Zeyu Fu:** Formal analysis, Investigation, Methodology, Validation. **Shiyuan Yang:** Formal analysis, Investigation, Methodology, Validation. **Yuning Zhou:** Formal analysis. **Huimin Zhu:** Formal analysis. **Yan Zhu:** Formal analysis. **Jia Zhou:** Formal analysis. **Kaili Lin:** Conceptualization, Funding acquisition, Project administration, Supervision, Writing - review & editing. **Yuanjin Xu:** Conceptualization, Funding acquisition, Investigation, Project administration, Supervision, Writing - review & editing.

Declaration of competing interest

The authors declare that they have no known competing financial interests or personal relationships that could have appeared to influence the work reported in this paper.

Data availability

The data that has been used is confidential.

Acknowledgements

This research was funded by the National Natural Science Foundation of China (82071082, 82370921), Fund of Department of Oral and Maxillofacial Surgery (Department 2023-01), Program of Shanghai Technology Research Leader (23XD1430800), Cross disciplinary Research Fund of Shanghai Ninth People's Hospital, Shanghai Jiao Tong university School of Medicine (JYJC202219), Shanghai's Top Priority Research Center (2022ZZ01017), and CAMS Innovation Fund for Medical Sciences (CIFMS, 2019-I2M-5–037).

Appendix A. Supplementary data

Supplementary data to this article can be found online at https://doi.org/10.1016/j.mtbio.2023.100906.

References

[1] B.L. Pihlstrom, B.S. Michalowicz, N.W. Johnson, Periodontal diseases, Lancet 366 (9499) (2005) 1809–1820.
[2] J.E. Deanfield, F. D'Aiuto, M. Czesnikiewicz-Guzik, Understanding residual inflammatory risk sheds new light on the clinical importance of periodontitis in cardiovascular disease, Eur. Heart J. 41 (7) (2020) 818–819.
[3] D.F. Kinane, P.G. Stathopoulou, P.N. Papapanou, Periodontal diseases, Nat. Rev. Dis. Prim. 3 (2017), 17038.
[4] A. Nasajpour, S. Ansari, C. Rinoldi, A.S. Rad, T. Aghaloo, S.R. Shin, Y.K. Mishra, R. Adelung, W. Swieszkowski, N. Annabi, A. Khademhosseini, A. Moshaverinia, A. Tamayol, A multifunctional polymeric periodontal membrane with osteogenic and antibacterial characteristics, Adv. Funct. Mater. 28 (3) (2018).
[5] X. Zheng, X. Ke, P. Yu, D. Wang, S. Pan, J. Yang, C. Ding, S. Xiao, J. Luo, J. Li, A facile strategy to construct silk fibroin based GTR membranes with appropriate mechanical performance and enhanced osteogenic capacity, J. Mater. Chem. B 8 (45) (2020) 10407–10415.
[6] N. Dubey, J.A. Ferreira, A. Daghrery, Z. Aytac, J. Malda, S.B. Bhaduri, M. C. Bottino, Highly tunable bioactive fiber-reinforced hydrogel for guided bone regeneration, Acta Biomater. 113 (2020) 164–176.
[7] D. Abdelaziz, A. Hefnawy, E. Al-Wakeel, A. El-Fallal, I.M. El-Sherbiny, New biodegradable nanoparticles-in-nanofibers based membranes for guided periodontal tissue and bone regeneration with enhanced antibacterial activity, J. Adv. Res. 28 (2021) 51–62.
[8] A. Kozlovsky, G. Aboodi, O. Moses, H. Tal, Z. Artzi, M. Weinreb, C.E. Nemcovsky, Bio-degradation of a resorbable collagen membrane (Bio-Gide) applied in a double-layer technique in rats, Clin. Oral Implants Res. 20 (10) (2009) 1116–1123.
[9] M.R. de Oliveira, S.M. Nabavi, N. Braidy, W.N. Setzer, T. Ahmed, S.F. Nabavi, Quercetin and the mitochondria: a mechanistic view, Biotechnol. Adv. 34 (5) (2016) 532–549.
[10] Y. Hu, Z. Gui, Y. Zhou, L. Xia, K. Lin, Y. Xu, Quercetin alleviates rat osteoarthritis by inhibiting inflammation and apoptosis of chondrocytes, modulating synovial macrophages polarization to M2 macrophages, Free Radic. Biol. Med. 145 (2019) 146–160.
[11] S. Teixeira, C. Siquet, C. Alves, I. Boal, M.P. Marques, F. Borges, J.L.F.C. Lima, S. Reis, Structure–property studies on the antioxidant activity of flavonoids present in diet, Free Radical Biol. Med. 39 (8) (2005) 1099–1108.
[12] M. Satué, M.d.M. Arriero, M. Monjo, J.M. Ramis, Quercitrin and Taxifolin stimulate osteoblast differentiation in MC3T3-E1 cells and inhibit osteoclastogenesis in RAW 264.7 cells, Biochem. Pharmacol. 86 (10) (2013) 1476–1486.
[13] C. Zhou, Y. Lin, Osteogenic differentiation of adipose-derived stem cells promoted by quercetin, Cell Prolif. 47 (2) (2014) 124–132.
[14] Y. Zhou, Y. Wu, W. Ma, X. Jiang, A. Takemra, M. Uemura, L. Xia, K. Lin, Y. Xu, The effect of quercetin delivery system on osteogenesis and angiogenesis under osteoporotic conditions, J. Mater. Chem. B 5 (3) (2017) 612–625.
[15] J.E. Song, N. Tripathy, D.H. Lee, J.H. Park, G. Khang, Quercetin inlaid silk fibroin/hydroxyapatite scaffold promotes enhanced osteogenesis, ACS Appl. Mater. Interfaces 10 (39) (2018) 32955–32964.
[16] J. Xue, T. Wu, Y. Dai, Y. Xia, Electrospinning and electrospun nanofibers: methods, materials, and applications, Chem. Rev. 119 (8) (2019) 5298–5415.
[17] C. Jia, D. Yu, M. Lamarre, P.L. Leopold, Y.D. Teng, H. Wang, Patterned electrospun nanofiber matrices via localized dissolution: potential for guided tissue formation, Adv. Mater. 26 (48) (2014) 8192–8197.
[18] M.C. Bottino, V. Thomas, G. Schmidt, Y.K. Vohra, T.M. Chu, M.J. Kowolik, G. M. Janowski, Recent advances in the development of GTR/GBR membranes for periodontal regeneration–a materials perspective, Dent. Mater. 28 (7) (2012) 703–721.
[19] Y. Zhang, N. Kong, Y. Zhang, W. Yang, F. Yan, Size-dependent effects of gold nanoparticles on osteogenic differentiation of human periodontal ligament progenitor cells, Theranostics 7 (5) (2017) 1214–1224.
[20] F. Shang, S. Liu, L. Ming, R. Tian, F. Jin, Y. Ding, Y. Zhang, H. Zhang, Z. Deng, Y. Jin, Human umbilical cord MSCs as new cell sources for promoting periodontal regeneration in inflammatory periodontal defect, Theranostics 7 (18) (2017) 4370–4382.
[21] J. Xie, H. Shen, G. Yuan, K. Lin, J. Su, The effects of alignment and diameter of electrospun fibers on the cellular behaviors and osteogenesis of BMSCs, Mater. Sci. Eng. C Mater. Biol. Appl. 120 (2021), 111787.
[22] J. Cui, X. Yu, B. Yu, X. Yang, Z. Fu, J. Wan, M. Zhu, X. Wang, K. Lin, Coaxially fabricated dual-drug loading electrospinning fibrous mat with programmed releasing behavior to boost vascularized bone regeneration, Adv. Healthcare Mater. 11 (16) (2022), e2200571.
[23] S. Faraji, N. Nowroozi, A. Nouralishahi, J. Shabani Shayeh, Electrospun polycaprolactone/graphene oxide/quercetin nanofibrous scaffold for wound dressing: evaluation of biological and structural properties, Life Sci. 257 (2020), 118062.
[24] L. Shang, Z. Liu, B. Ma, J. Shao, B. Wang, C. Ma, S. Ge, Dimethyloxallyl glycine/nanosilicates-loaded osteogenic/angiogenic difunctional fibrous structure for functional periodontal tissue regeneration, Bioact. Mater. 6 (4) (2021) 1175–1188.
[25] S. He, Q. Hu, Y. Sun, Y. Xu, L. Huang, G. Cao, T. Guo, Electrospun polycaprolactone incorporated with fluorapatite nanoparticles composite scaffolds enhance healing of experimental calvarial defect on rats, Ann. Transl. Med. 11 (9) (2023) 313.
[26] X. Liu, X. He, D. Jin, S. Wu, H. Wang, M. Yin, A. Aldalbahi, M. El-Newehy, X. Mo, J. Wu, A biodegradable multifunctional nanofibrous membrane for periodontal tissue regeneration, Acta Biomater. 108 (2020) 207–222.
[27] S. Ren, Y. Zhou, K. Zheng, X. Xu, J. Yang, X. Wang, L. Miao, H. Wei, Y. Xu, Cerium oxide nanoparticles loaded nanofibrous membranes promote bone regeneration for periodontal tissue engineering, Bioact. Mater. 7 (2022) 242–253.
[28] F. Doustdar, S. Ramezani, M. Ghorbani, F. Mortazavi Moghadam, Optimization and characterization of a novel tea tree oil-integrated poly (epsilon-caprolactone)/soy protein isolate electrospun mat as a wound care system, Int. J. Pharm. 627 (2022), 122218.
[29] P. He, Q. Zhong, Y. Ge, Z. Guo, J. Tian, Y. Zhou, S. Ding, H. Li, C. Zhou, Dual drug loaded coaxial electrospun PLGA/PVP fiber for guided tissue regeneration under control of infection, Mater. Sci. Eng. C Mater. Biol. Appl. 90 (2018) 549–556.
[30] S. Liu, Y.N. Wang, B. Ma, J. Shao, H. Liu, S. Ge, Gingipain-responsive thermosensitive hydrogel loaded with SDF-1 facilitates in situ periodontal tissue regeneration, ACS Appl. Mater. Interfaces 13 (31) (2021) 36880–36893.
[31] N. Dubey, J.A. Ferreira, A. Daghrery, Z. Aytac, J. Malda, S.B. Bhaduri, M. C. Bottino, Highly tunable bioactive fiber-reinforced hydrogel for guided bone regeneration, Acta Biomater. 113 (2020) 164–176.
[32] B. Yi, Y. Shen, H. Tang, X. Wang, B. Li, Y. Zhang, Stiffness of aligned fibers regulates the phenotypic expression of vascular smooth muscle cells, ACS Appl. Mater. Interfaces 11 (7) (2019) 6867–6880.
[33] M. Lian, Y. Han, B. Sun, L. Xu, X. Wang, B. Ni, W. Jiang, Z. Qiao, K. Dai, X. Zhang, A multifunctional electrowritten bi-layered scaffold for guided bone regeneration, Acta Biomater. 118 (2020) 83–99.
[34] M. Lian, B. Sun, Z. Qiao, K. Zhao, X. Zhou, Q. Zhang, D. Zou, C. He, X. Zhang, Bi-layered electrospun nanofibrous membrane with osteogenic and antibacterial properties for guided bone regeneration, Colloids Surf. B Biointerfaces 176 (2019) 219–229.
[35] S. Liu, X. Yan, J. Guo, H. An, X. Li, L. Yang, X. Yu, S. Li, Periodontal ligament-associated protein-1 knockout mice regulate the differentiation of osteoclasts and osteoblasts through TGF-beta1/Smad signaling pathway, J. Cell. Physiol. (2023).
[36] T.J. Ji, B. Feng, J. Shen, M. Zhang, Y.Q. Hu, A.X. Jiang, D.Q. Zhu, Y.W. Chen, W. Ji, Z. Zhang, H. Zhang, F. Li, An avascular niche created by axitinib-loaded PCL/collagen nanofibrous membrane stabilized subcutaneous chondrogenesis of mesenchymal stromal cells, Adv. Sci. (2021), e2100351.
[37] X. Lan, H. Wang, J. Bai, X. Miao, Q. Lin, J. Zheng, S. Ding, X. Li, Y. Tang, Multidrug-loaded electrospun micro/nanofibrous membranes: fabrication strategies, release behaviors and applications in regenerative medicine, J. Contr. Release 330 (2021) 1264–1287.

[38] A. Denchai, D. Tartarini, E. Mele, Cellular response to surface morphology: electrospinning and computational modeling, Front. Bioeng. Biotechnol. 6 (2018) 155.
[39] P.K. Mattila, P. Lappalainen, Filopodia: molecular architecture and cellular functions, Nat. Rev. Mol. Cell Biol. 9 (6) (2008) 446–454.
[40] J.W. Jang, K.E. Min, C. Kim, C. Wern, S. Yi, PCL and DMSO(2) composites for bio-scaffold materials, Materials 16 (6) (2023).
[41] Y. Li, J. Yao, C. Han, J. Yang, M.T. Chaudhry, S. Wang, H. Liu, Y. Yin, Quercetin, inflammation and immunity, Nutrients 8 (3) (2016) 167.
[42] A. Bharadwaz, A.C. Jayasuriya, Recent trends in the application of widely used natural and synthetic polymer nanocomposites in bone tissue regeneration, Mater. Sci. Eng. C Mater. Biol. Appl. 110 (2020), 110698.
[43] J. Caballe-Serrano, K. Sawada, R.J. Miron, D.D. Bosshardt, D. Buser, R. Gruber, Collagen barrier membranes adsorb growth factors liberated from autogenous bone chips, Clin. Oral Implants Res. 28 (2) (2017) 236–241.
[44] Y. Zhou, Y. Wu, X. Jiang, X. Zhang, L. Xia, K. Lin, Y. Xu, The effect of quercetin on the osteogenesic differentiation and angiogenic factor expression of bone marrow-derived mesenchymal stem cells, PLoS One 10 (6) (2015), e0129605.
[45] A. Padhi, A.H. Thomson, J.B. Perry, G.N. Davis, R.P. McMillan, S. Loesgen, E. N. Kaweesa, R. Kapania, A.S. Nain, D.A. Brown, Bioenergetics underlying single-cell migration on aligned nanofiber scaffolds, Am. J. Physiol. Cell Physiol. 318 (3) (2020) C476–C485.
[46] J.I. Sasaki, G.L. Abe, A. Li, P. Thongthai, R. Tsuboi, T. Kohno, S. Imazato, Barrier membranes for tissue regeneration in dentistry, Biomater. Investig. Dent. 8 (1) (2021) 54–63.
[47] M.M. Hasani-Sadrabadi, P. Sarrion, N. Nakatsuka, T.D. Young, N. Taghdiri, S. Ansari, T. Aghaloo, S. Li, A. Khademhosseini, P.S. Weiss, A. Moshaverinia, Hierarchically patterned polydopamine-containing membranes for periodontal tissue engineering, ACS Nano 13 (4) (2019) 3830–3838.
[48] N. Wang, L. Wang, J. Yang, Z. Wang, L. Cheng, Quercetin promotes osteogenic differentiation and antioxidant responses of mouse bone mesenchymal stem cells through activation of the AMPK/SIRT1 signaling pathway, Phytother Res. 35 (5) (2021) 2639–2650.